Chromatin interaction of TATA-binding protein is dynamically regulated in human cells

Petra de Graaf[1], Florence Mousson[1], Bart Geverts[2], Elisabeth Scheer[3], Laszlo Tora[3], Adriaan B. Houtsmuller[2] and H. Th. Marc Timmers[1,*]

[1]Department of Physiological Chemistry and Netherlands Proteomic Center, University Medical Centre Utrecht, Universiteitsweg 100, 3584 CG Utrecht, Netherlands
[2]Department of Pathology, Josephine Nefkens Institute, Erasmus MC, 3000 CA Rotterdam, Netherlands
[3]Department of Functional Genomics, Institut de Génétique et de Biologie Moléculaire et Cellulaire (IGBMC), UMR 7104 CNRS, UdS, INSERM U964, BP 10142, F-67404 ILLKIRCH Cedex, CU de Strasbourg, France
*Author for correspondence (h.t.m.timmers@umcutrecht.n)

Accepted 27 April 2010
Journal of Cell Science 123, 2663-2671

doi:10.1242/jcs.064097

Summary

Gene transcription in mammalian cells is a dynamic process involving regulated assembly of transcription complexes on chromatin in which the TATA-binding protein (TBP) plays a central role. Here, we investigate the dynamic behaviour of TBP by a combination of fluorescence recovery after photobleaching (FRAP) and biochemical assays using human cell lines of different origin. The majority of nucleoplasmic TBP and other TFIID subunits associate with chromatin in a highly dynamic manner. TBP dynamics are regulated by the joint action of the SNF2-related BTAF1 protein and the NC2 complex. Strikingly, both BTAF1 and NC2 predominantly affect TBP dissociation rates, leaving the association rate unchanged. Chromatin immunoprecipitation shows that BTAF1 negatively regulates TBP and NC2 binding to active promoters. Our results support a model for a BTAF1-mediated release of TBP-NC2 complexes from chromatin.

Key words: Basal transcription factors, Gene expression, FRAP, TFIID, TBP

Introduction

Gene transcription is a dynamic process involving a continuous assembly and disassembly of the transcription complexes on gene promoters (Hager et al., 2009; Sikorski and Buratowski, 2009). Live-cell imaging combined with fluorescence recovery after photobleaching (FRAP) has revealed a high mobility and transient chromatin interactions for a variety of transcription factors involved in RNA polymerase II (pol II)-mediated transcription (Farla et al., 2004; Farla et al., 2005; Hager et al., 2009; Hoogstraten et al., 2002; Karpova et al., 2008; McNally et al., 2000; Mueller et al., 2008; Muller et al., 2001; Sprouse et al., 2008; Stenoien et al., 2001; van Royen et al., 2009). The *Drosophila* heat shock factor is an exception to this and shows a slow recovery under heat shock conditions (Yao et al., 2006).

Tagging the largest catalytic subunit of pol II with green fluorescent protein (GFP) revealed that ~75% of this enzyme moved rapidly in living cells, whereas 25% was transiently immobile and active in transcription, as this fraction disappeared after transcription inhibition (Kimura et al., 2002). Kinetic measurements of the different steps in the pol II transcription cycle indicate that formation of the pre-initiation complex (PIC) is very dynamic and rather inefficient, with only a small fraction of the initiated pol II proceeding to elongation (Darzacq et al., 2007). This is in agreement with recent findings of promoter-proximal pausing of pol II as a rather general step in the transition to productive elongation (Core and Lis, 2008). Visualization of native mRNA transcripts indicates that elongating pol II proceeds with a rate ranging from 1.5-2.0 kb/minute (Boireau et al., 2007; Yao et al., 2007) to 4.3 kb/minute (Darzacq et al., 2007).

Detailed analysis of the pol I transcription complex shows that pol I is dynamically imported into the nucleolus (Dundr et al., 2002) and when higher levels of transcription are required, assembly of pol I complexes is more efficient and the rate of entry into elongation is elevated (Gorski et al., 2008).

The TATA-binding protein (TBP) plays a central role in eukaryotic transcription by all three RNA polymerases and resides in at least four transcription complexes: TFIID, B-TFIID, SL1 and TFIIIB (for reviews, see Burley and Roeder, 1996; Muller et al., 2007; Pereira et al., 2003; Thomas and Chiang, 2006). In TFIID, TBP is associated with 13-14 evolutionary conserved TBP-associated factors (TAFs) (Tora, 1992). B-TFIID represents the most abundant TBP-containing complex and consists of TBP and a single TAF, BTAF1, which is a conserved member of the SNF2 ATPases family (Pereira et al., 2003). In cellular lysates TBP is stably associated in the TFIID, TFIIIB and SL1 complexes, but TBP and BTAF1 are exchanging rapidly (Mousson et al., 2008). DNA-bound TBP provides the platform for association of basal transcription factors and pol II to direct formation of a functional PIC. TBP-DNA complexes can also be recognized efficiently by the negative co-factor NC2, which can inhibit in vitro transcription by blocking association of the basal factors TFIIA and TFIIB (Goppelt et al., 1996; Inostroza et al., 1992; Meisterernst et al., 1991). Interestingly, both biochemical and genomic experiments point to a functional interplay between BTAF1 (or its yeast orthologue Mot1p) and NC2 (Geisberg et al., 2002; Hsu et al., 2008; Klejman et al., 2004; van Werven et al., 2008).

TBP dynamics have been studied by FRAP both in living human cells (HeLa) (Chen et al., 2002), and in yeast (Sprouse et al., 2008), with strikingly different results. In the HeLa cell system, a slow recovery (>20 minutes) was measured, indicating a large immobile fraction of TBP, which most probably involves chromatin binding (Chen et al., 2002). This is in contrast to yeast TBP, which

shows a remarkable fast FRAP (less than 15 seconds), but not as rapid as TFIIB or TAF1 (Sprouse et al., 2008). Besides different model systems, another difference between the two studies is the method of expressing GFP-tagged TBP. In the human system, a transient overexpression system was used, whereas in yeast the genes for TBP, TFIIB and TAF1 were replaced by fluorescently tagged versions.

Here, we investigate the dynamics of TBP in living human cells by using a retroviral transduction to express stably GFP-TBP to near-endogenous levels. Analysis of these cell lines by fluorescence recovery after photobleaching reveals that the major fraction of TBP fluorescence recovers rapidly, which is indicative of a dynamic interaction with chromatin. In a combination of siRNA-mediated knockdown and transient overexpression experiments, we find that the NC2 complex stabilizes chromatin association of TBP, whereas BTAF1 promotes its release. Chromatin immunoprecipitation experiments confirm that BTAF1 controls the promoter-bound fraction of TBP and NC2. Our findings support a model for a dynamic control of basal transcription factor complexes to allow rapid transcriptional responses of cells to internal and external cues.

Results

GFP-TBP is partly bound to chromatin in living cells

To study TBP dynamics in vivo, we generated cell lines expressing GFP-tagged human TBP by retroviral transduction. Confocal microscope images of monoclonal cell lines derived from human U2OS osteosarcoma or HeLa cervix carcinoma cells showed that, as expected, GFP-TBP is present in the nucleus and its pattern overlaps with DNA staining (Fig. 1A). To ensure that the GFP moiety does not affect TBP function, extracts of the generated cell lines were analyzed for expression and incorporation of GFP-TBP into TBP-containing complexes. Gel filtration and immunoprecipitation analyses indicated that GFP-TBP is efficiently incorporated in both B-TFIID and TFIID complexes (supplementary material Fig. S1A-C). Furthermore, the analyses show that GFP-TBP is expressed at near endogenous levels in HeLa- and U2OS-derived cell lines. We used the GFP-TBP cell lines to analyze the behaviour of TBP by fluorescent recovery after photobleaching (FRAP). As controls, we compared FRAP curves of GFP-TBP with those of GFP fused to histone H2B (H2B-GFP) or to the SV40 nuclear localization signal (NLS-GFP). FRAP experiments were performed by bleaching a narrow strip (~0.75 μm) covering the nucleoplasm across the width of the nucleus and recording the recovery of fluorescence in this strip every 21 mseconds (van Royen et al., 2009; Xouri et al., 2007). As expected, the recovery of NLS-GFP fluorescence was very rapid and no immobile fraction could be detected, whereas H2B-GFP was largely immobile (80-90%) in the strip-FRAP experiments. GFP-TBP fluorescence in both HeLa- and U2OS-derived cells displayed a rapid initial recovery followed by a slower subsequent phase (Fig. 1B). A sequence of frames depicting the whole nucleus after bleaching shows similar results: no recovery for H2B-GFP, partial recovery for GFP-TBP and full recovery for NLS-GFP (supplementary material Fig. S2). To analyze experimental FRAP curves, a large database was constructed, which contained FRAP curves generated by Monte Carlo computer simulations (see Materials and Methods for a detailed description). Each curve in this database represents a scenario with a specific diffusion coefficient and a specific k_{on} and k_{off} representing the rate at which proteins bind to and release from immobile DNA (e.g. Xouri et al., 2007). Each experimental FRAP curve was compared with the computer-generated curves of the database using standard ordinary least square fitting. From this, the ten best-fitting curves were taken to calculate the average diffusion coefficients and rate

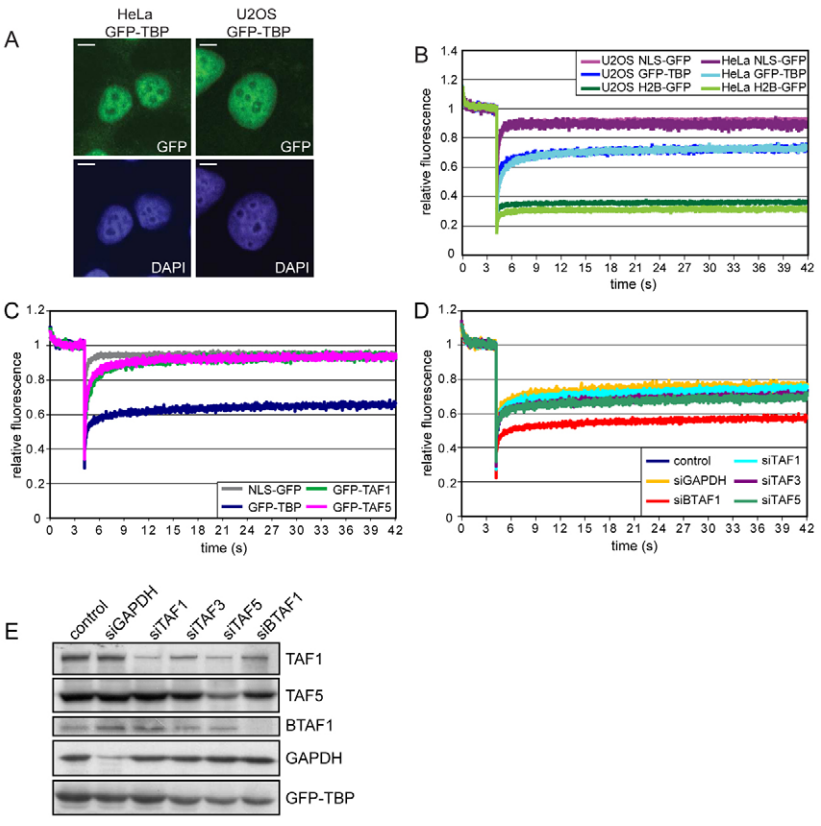

Fig. 1. Dynamics of TBP and TFIID-TAFs in living cells. (**A**) Confocal microscopic images of GFP-TBP-expressing HeLa (left) or U2OS (right) cell lines indicate nuclear localization of GFP-TBP. GFP signals are in green (upper panels) and DAPI signals for DNA-staining in blue (lower panels). Scale bars, 5 μm. (**B**) HeLa tk$^-$ and U2OS cells expressing GFP-TBP (respectively light and dark blue), NLS-GFP (respectively pink and purple) or H2B-GFP (respectively light and dark green) were analyzed for FRAP by CLSM. Prior to photo-bleaching, a strip spanning the nucleus was scanned at low laser power. After this, the ROI was scanned every 21 mseconds until 38 seconds after bleaching. Raw data were normalized for fluorescence intensity before bleaching and an average of 10 nuclei was plotted. (**C**) ts013 cells expressing GFP-TAF1 and U2OS cells expressing GFP-TAF5 were analyzed for FRAP as described in B. U2OS cells expressing NLS-GFP and GFP-TBP were included as a reference. Incorporation of the tagged TAFs into TFIID was shown by immunoprecipitation experiments (supplementary material Fig. S1D,E). (**D**) U2OS GFP-TBP cells were transfected with RNAi oligos as indicated and analyzed for FRAP as described in B. Transfection efficiency of the RNAi oligos was analysed by co-transfecting siGLO red (supplementary material Fig. S3). (**E**) Knockdown efficiency was analyzed in total lysates of the transfected cells as described in D by immunoblotting with TAF1, BTAF1, TAF5, GAPDH and GFP antibodies. Knockdown of TAF3 was efficient as measured by RT-PCR (data not shown).

constants. The values for diffusion coefficient and rate constants determined in this way are summarized for all experiments in supplementary material Table S1. Note that on- and off-rate constants correspond directly to the (transiently-) immobile fraction (see Materials and Methods). The HeLa- and U2OS-derived GFP-TBP cell lines yielded similar results. In both cell lines, ~70% of the GFP-TBP recovers rapidly and the characteristic time spent in the subsequent transiently immobile state was 2-3 minutes (supplementary material Table S1).

TFIID components interact very transiently with chromatin

These observations raise the issue of the dynamics of the TFIID complex, consisting of TBP and 13-14 TAFs (Burley and Roeder, 1996; Muller et al., 2007; Thomas and Chiang, 2006). To investigate this, we tagged different TFIID-TAFs with GFP. First, GFP-tagged TAF1 was stably expressed in the hamster ts013 cell line, which expresses a temperature-sensitive mutant of TAF1 (Sekiguchi et al., 1991). The majority of GFP-TAF1 recovered rapidly after bleaching with a small transiently immobile fraction (~18%) (Fig. 1C; supplementary material Table S1). It is important to note that FRAP of GFP-TAF1 is slower than the NLS-GFP, indicating a short residence time to chromatin. Second, a GFP-tagged version of TAF5, one of the structural TAFs (Cler et al., 2009; Leurent et al., 2004), was stably expressed in U2OS cells. TAF5 exhibited a similar recovery to TAF1 in the FRAP analysis (Fig. 1C; supplementary material Table S1). Thus, the TAFs of TFIID are highly mobile in vivo, with a small proportion displaying short interaction times with chromatin (1-2 sec, supplementary material Table S1).

Effect of TAFs and BTAF1 expression on TBP dynamics

Given the association of TBP with the TFIID complex, we investigated whether TAFs determine the dynamic interaction of TBP with chromatin. We selected three different TFIID TAFs for siRNA-mediated knockdown: TAF1, which interacts with TBP (Takada et al., 1992); TAF3, which anchors TFIID to methylated histones (Vermeulen et al., 2007); and the structural TAF5 (Leurent et al., 2004). To ensure that the single cells analyzed by FRAP were transfected by siRNAs, a transfection indicator was included as described in the Materials and Methods (supplementary material Fig. S3). The majority of cells were transfected, as also indicated by a reduction in protein levels (Fig. 1E). Knockdown of TAF1, TAF3 or TAF5 expression did not significantly change the dynamics of TBP (Fig. 1D). Similarly, a reduced expression of the TBP-associating factor BRF1 from the TFIIIB complex involved in pol III transcription did not influence TBP dynamics (supplementary material Fig. S4). By contrast, siRNA knockdown of BTAF1, the single TAF in the B-TFIID complex (Timmers et al., 1992), reduced the mobile fraction of TBP from 70% to less than 50% (Fig. 1D; supplementary material Table S1). Similar results were obtained upon inducible shRNA knockdown of BTAF1 (supplementary material Fig. S5). From these experimental FRAP curves, both the dissociation rate constant k_{off} and association rate constant k_{on} were determined (see Materials and Methods for a detailed description). Interestingly, k_{off} decreased when BTAF1 was downregulated, whereas k_{on} did not change significantly (supplementary material Table S1), suggesting that BTAF1 regulates the release of TBP from chromatin and not its association. To further investigate the role of BTAF1 in TBP-chromatin interaction, we determined the mobility of TBP upon BTAF1 overexpression. To this end, GFP-TBP was transfected with or without HA-tagged BTAF1 in 293T cells and the resulting cells were subjected to FRAP analysis. Overexpression of BTAF1 increased the mobile fraction of GFP-TBP (Fig. 2A,B).

Having established that BTAF1 function is important for TBP dynamics, we investigated involvement of BTAF1 in global chromatin association of TBP by biochemical fractionation of cell extracts. Therefore, nuclear proteins were selectively extracted from inducible BTAF1 knockdown cells and analyzed by immunoblotting. The chromatin-bound fraction of TBP was specifically increased upon reduction of BTAF1 expression (Fig. 3). As expected, histone H4 could be detected only in the chromatin-enriched fractions. Little effect was observed on the distribution of the TAF1 and TAF5 subunits of TFIID, indicating that BTAF1 regulates chromatin binding of TBP without affecting the TAF subunits of TFIID. This hypothesis is strengthened by the observation that the dynamic behaviour of TAF5 is not affected by BTAF1 knockdown (data not shown).

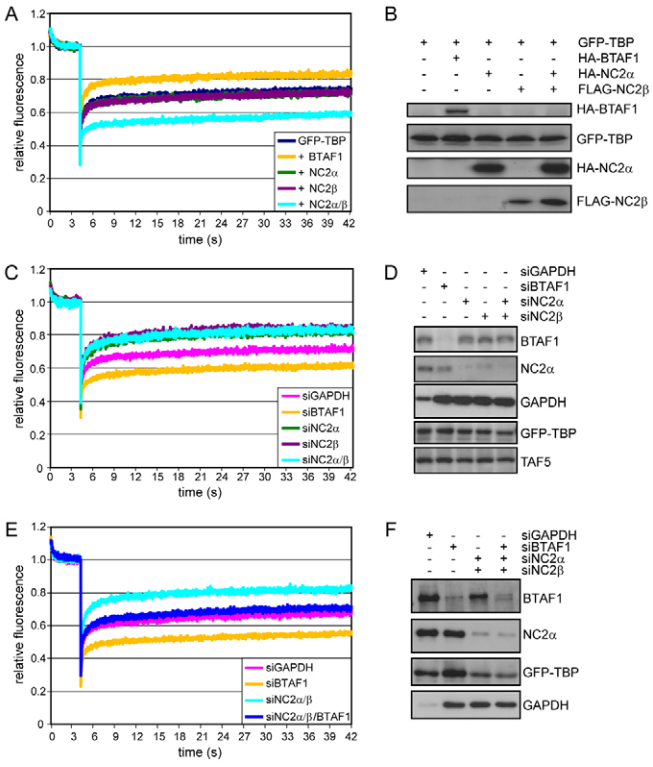

Fig. 2. Chromatin association of GFP-TBP is differentially regulated by NC2 complex and BTAF1. (**A**) HEK293T cells were transfected with pEGFP-TBP (25 ng) and subsequently pMT2-SM HA-BTAF1 wt (2 µg), pCMV HA-NC2α (250 ng), pCMV FLAG-NC2β (250 ng) as indicated. Mock DNA (pMT2-SM) was added to have equal amounts of plasmid per transfection. Cells were analyzed for FRAP 20 hours after transfection. Quantification of FRAP signals was performed as described in Fig. 1B. (**B**) Expression levels of the exogenous protein as described in A was analyzed in total lysates by immunoblotting with HA, FLAG and GFP antibodies. (**C**) U2OS GFP-TBP-expressing cells were transfected with RNAi oligos as indicated and analyzed for FRAP as described in Fig. 1B. (**D**) Knockdown efficiency was analyzed in total lysates of the transfected cells as described in C by immunoblotting with BTAF1, NC2α, GAPDH, GFP and TAF5 antibodies. (**E**) U2OS GFP-TBP expressing cells were transfected with RNAi oligos as indicated and analyzed for FRAP as described in Fig. 1B. (**F**) Knockdown efficiency was analyzed in total lysates of the transfected cells as described in E by immunoblotting with BTAF1, NC2α, GAPDH and GFP antibodies.

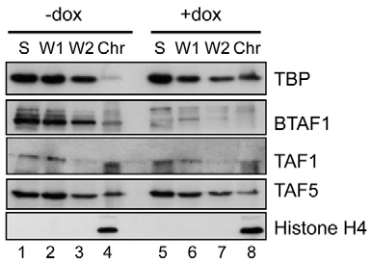

Fig. 3. BTAF1 knockdown increases chromatin association of TBP. Nuclear fractions were prepared from HeLa TR^{s} shBTAF1 cells treated with or without doxycycline for 8 days as described in the Materials and Methods. Soluble fraction, washes and soluble chromatin fraction were analyzed immunoblotting with TBP, BTAF1, TAF1, TAF5 and histone H4 antibodies.

NC2 regulates TBP-chromatin interaction

The negative co-factor NC2 interacts with DNA-bound TBP with a high affinity (Gilfillan et al., 2005). Several observations indicate that BTAF1 and its yeast ortholog Mot1p overlap in function with NC2 (Geisberg et al., 2002; Klejman et al., 2004; van Werven et al., 2008). Thus, NC2 may also play a role in regulation of TBP interaction to chromatin in human cells. Interestingly, knockdown of NC2 expression increases the fraction of mobile TBP molecules in the GFP-TBP U2OS cells (Fig. 2C). Remarkably, knockdown of the NC2β subunit also reduced the expression of the NC2α subunit in total lysates (Fig. 2D). This strengthens the notion that NC2α and NC2β act as a complex to regulate TBP. As shown before, BTAF1 knockdown reduced the mobile fraction (supplementary material Table S1). The opposing effects of NC2 and BTAF1 on TBP binding to chromatin are corroborated by the combined knockdown of NC2 and BTAF1, which reverted the dynamics of TBP to that of untreated cells (Fig. 2E,F). These results predict that overexpression of the NC2 complex may increase chromatin association of TBP in cells. Indeed, the fraction of mobile TBP is reduced only when both subunits of NC2 are overexpressed (Fig. 2A), which again indicates that they act as a complex. Furthermore, we could show that overexpression of TBP increased the chromatin binding of both GFP-NC2α and GFP-NC2β (Fig. 5), which strengthens our hypothesis that NC2 controls the binding of TBP to chromatin.

This set of experiments allowed us to also determine the effect of NC2 on the k_{on} and k_{off} of the TBP-chromatin interaction. Strikingly, only the k_{off} changes after reduction or overexpression of NC2 complex (Fig. 4A; supplementary material Table S1), whereas the k_{on} does not change significantly (Fig. 4B). Comparison with the effects of BTAF1 (Fig. 4A) reveals that BTAF1 and NC2 have opposite effects on the dissociation rate of TBP from chromatin. We used our computer modelling to illustrate the effect of altering k_{on} or k_{off} on FRAP curves. The FRAP curves depicted in Figs 1 and 2 clearly fit better to curves representing scenarios where only k_{off} is varied (Fig. 4C) compared with scenarios where only k_{on} changes (Fig. 4D).

BTAF1 regulates TBP and NC2α levels at promoters

FRAP analysis indicated that BTAF1 and the NC2 complex act in concert to regulate the dynamic behaviour of TBP in cells. To explore the influence of BTAF1 on promoter binding of TBP and NC2, we performed chromatin immunoprecipitation (ChIP) experiments in cells with a reduced BTAF1 expression. We selected a set of highly expressed genes for this analysis. As expected, TBP binding peaks at the transcription start sites (TSS) of the genes encoding ribosomal proteins *RPL31*, *RPL34* and *RPS10*, and the shared promoter of the divergent histone *H2BJ* and *H2AG* genes (Fig. 6B; supplementary material Fig. S6). BTAF1 knockdown results in increased TBP binding at the promoter of all three loci. This is further supported by ChIP sequencing data for TBP, comparing GAPDH with BTAF1 knockdown using siRNA (Johannes et al., 2010). Of the genomic regions increased in TBP binding by BTAF1 knockdown 70% correspond to promoter regions. This indicates that the effect of BTAF1 on TBP binding is very general to pol II promoters (Johannes et al., 2010). Interestingly, the ChIP experiments in Fig. 6C show a strong

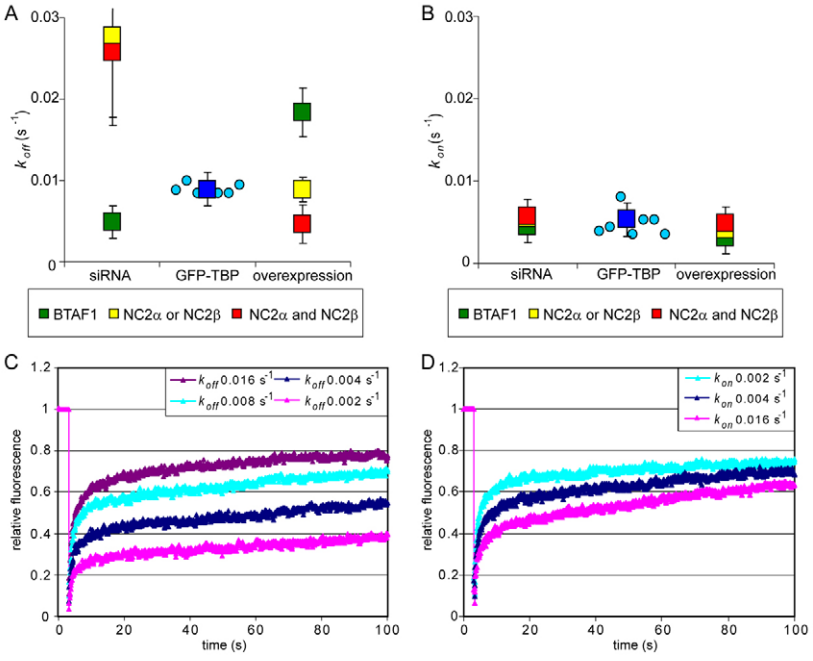

Fig. 4. BTAF1 and NC2α affect dissociation rates of TBP from chromatin. (**A**,**B**) Graphs showing the dissociation and association rates of TBP (k_{on} and k_{off}), as determined by computer modelling-based analysis, after either downregulation or overexpression of BTAF1 (green squares), NC2α or NC2β (yellow squares), or NC2α and NCβ (red squares) compared with untreated cells (blue squares). In addition, the variation of individual control experiments performed in parallel with downregulation and overexpression experiments is shown (blue circles). The experiments in which either NC2α or NC2β expression level was manipulated were averaged for clarity as they showed similar reproducible results. Mean and standard deviations (as shown with the error bars) were calculated from 2-10 biological independent experiments. (**C**) FRAP curves representing a scenario where k_{on} was constant (0.004 s^{-1}) and k_{off} was varied (0.016, 0.008, 0.004 and 0.002 s^{-1}), resulting in both increase of immobile fraction and residence time. (**D**) FRAP curves representing a scenario where k_{off} was constant (0.008 s^{-1}) and k_{on} was varied (0.002, 0.004 and 0.016 s^{-1}). As residence time depends on k_{off} only, in this scenario only the immobile fraction varies with varying k_{on}.

increase of promoter binding by NC2α after reduction of BTAF1 expression (see also supplementary material Fig. S6C). These data support a model in which BTAF1 counteracts the effect of NC2, as observed in the FRAP experiments. This is agreement with biochemical experiments in yeast, which suggested that Mot1p-NC2-TBP-DNA represents a transcriptionally silent complex (van Werven et al., 2008). To analyze whether the increased association of TBP and NC2α has transcriptional consequences pol II binding was measured by ChIP. Binding of pol II is not altered after BTAF1 knockdown (Fig. 6D). To confirm this, mRNA expression of these genes was analyzed by reverse transcription qPCR. The increased binding of TBP did not enhance mRNA levels; *RPL31*, *RPS10*, *H2A* and *H2B* mRNAs are not influenced by BTAF1 knockdown, whereas *RPL34* expression is reduced to ~60% (Fig. 6E; supplementary material Fig. S6D). The limited effect of BTAF1 on transcription is consistent with mRNA profiling of BTAF1 knockdown cells (data not shown). Taken together, these analyses indicate that an increased association of TBP and NC2 to promoters does not lead to increased mRNA transcript levels.

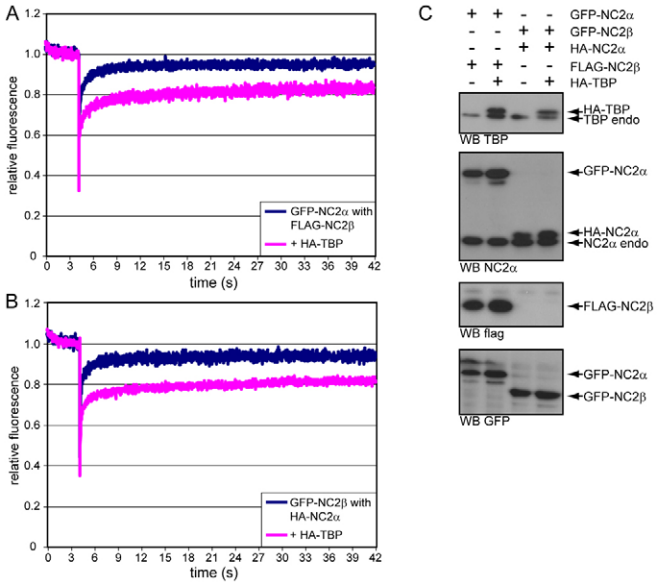

Fig. 5. Chromatin association of GFP-NC2 is regulated by TBP. (**A**) HEK293T cells were transfected with pEGFP-NC2α (100 ng) and pCMV-flag-NC2β (200 ng) with or without pMT2-SM HA-TBP (1.7 µg). Mock DNA (pMT2-SM) was added to ensure equal amounts of plasmid were present per transfection. Cells were analyzed for FRAP 20 hours after transfection. (**B**) HEK293T cells were transfected with pEGFP-NC2β (100 ng) and pCMV-HA-NC2α (200 ng) with or without pMT2-SM HA-TBP (1.7 µg). Mock DNA (pMT2-SM) was added to have equal amounts of plasmid per transfection. Cells were analyzed for FRAP 20 hours after transfection. (**C**) Protein expression was analyzed in total lysates of the transfected cells as described in A,B by immunoblotting with TBP, NC2α, FLAG and GFP antibodies.

Discussion

In this study, we combined live-cell imaging and biochemical approaches to investigate the molecular mechanisms involved in the dynamic behaviour of human basal transcription factor TBP. FRAP experiments show that a significant fraction of TBP is transiently immobilized on the chromatin, but the majority of TBP is mobile. Part of this mobile pool may represent the TFIID complex. The TAF1 and TAF5 subunits of TFIID interact only shortly with chromatin (1-2 seconds) and most of these proteins are represented in the mobile fraction. The mobile fraction of TBP is regulated by BTAF1 and by NC2 expression. Either downregulation of BTAF1 or overexpression of NC2 decreases the mobile fraction and increases the part of TBP, which is transiently immobile on chromatin. Conversely, knockdown of NC2 or overexpression of BTAF1 increases the mobile fraction. Interestingly, computer-based analysis of the FRAP data suggests that the observed changes in TBP dynamics by BTAF1 and NC2 depend only on changes in dissociation of TBP from the chromatin, leaving association rates unchanged.

The results of our study are largely similar to recent findings in yeast, which indicated that TBP is a rather mobile protein (Sprouse et al., 2008). By contrast, in a previous study of human cells, Chen et al. reported a large immobile fraction of GFP-TBP upon transient overexpression, which displayed residence times of ~20 minutes (Chen et al., 2002). ATP depletion increased the chromatin binding of transfected GFP-TBP even further, which would be consistent with involvement of the ATPase function of BTAF1. Besides technical differences in the FRAP setup, we propose that the differences between the studies relate to the overexpression versus stable expression of GFP-TBP as overexpression of TBP could titrate out BTAF1 and/or NC2. Indeed, when we transiently express GFP-TBP in U2OS cells, we observe an increase in chromatin binding when transfecting higher amounts of GFP-TBP (supplementary material Fig. S7). Additional support for this is that, in contrast to Chen et al. (Chen et al., 2002), we do not observe GFP-TBP localization to the mitotic chromosomes, which is consistent with findings with endogenous proteins [Kieffer-Kwon et al. (Kieffer-Kwon et al., 2004) and data not shown].

Although the TBP, BTAF1/Mot1p and NC2 proteins are highly conserved throughout evolution, the molecular mechanisms by which they perform their function might be slightly different between organisms. In yeast cells, TBP-YFP fluorescence fully recovered within 15 seconds after bleaching with no detectable immobile fraction (Sprouse et al., 2008). Importantly, TBP-YFP was expressed from the endogenous locus. Interestingly, the dynamics of yeast TBP are reduced in a *mot1* mutant (Sprouse et al., 2008). No effect on TBP mobility was observed in a yeast NC2α (*bur6*) mutant strain, whereas reduction of TAF1 (*taf1*) slightly increased TBP mobility (Sprouse et al., 2008). By contrast, we observed in human cells that TBP dynamics are differentially regulated by BTAF1 and NC2, whereas reduced expression of TAF1 or other TFIID-TAFs has no effect on the dynamic association of TBP with the chromatin.

The heterodimeric NC2 repressor complex has been shown in vitro to increase binding of TBP to promoter and non-promoter DNA, and to stabilize TBP-DNA complexes in general (Gilfillan et al., 2005; Goppelt et al., 1996). Experiments in vitro indicated that human BTAF1 and NC2 can compete for binding to DNA-bound TBP (Klejman et al., 2004). In addition, genome-wide location analyses in yeast indicate that Mot1p and NC2 bind to an overlapping set of promoters (van Werven et al., 2008). Biochemical analysis of chromatin complexes resulted in isolation of a stable Mot1p-NC2-TBP-TATA complex (van Werven et al., 2008), which could be disrupted by the addition of ATP. By contrast, analyses of human chromatin failed to identify a stable BTAF1-NC2-TBP-DNA complex [Gilfillan et al. (Gilfillan et al., 2005) and data not shown].

Our observations that modulating NC2 expression selectively affects the dissociation constant of TBP (Fig. 4) fits with the

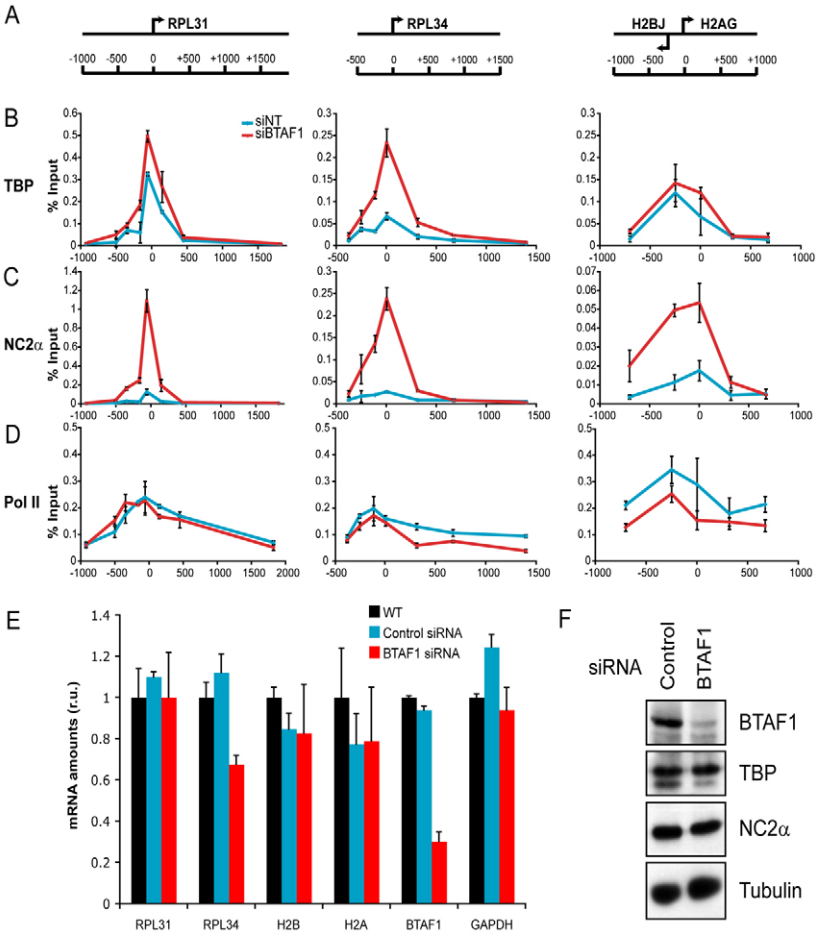

Fig. 6. BTAF1 regulates TBP and NC2α levels at promoters. (**A**) Schematic representation of the genes *rpl31*, *rpl34* and the *hist1h2bjh2ag* locus. The numbers correspond to the graphs represented in B-D. (**B**) Chromatin immunoprecipitation (ChIP) from HeLa tk⁻ cells transfected with siRNA targeting BTAF1 or control siRNA followed by quantitative PCR. Signals are plotted as percentage of input for precipitation with TBP (SL30) antibody. The data shown are representative of a triplicate. (**C**) ChIP followed from HeLa tk⁻ cells transfected with siRNA targeting BTAF1 or control siRNA by quantitative PCR. Signals are plotted as percentage of input for precipitation with NC2α antibody. The data shown are representative of a triplicate. (**D**) ChIP followed from HeLa tk⁻ cells transfected with siRNA targeting BTAF1 or control siRNA by quantitative PCR. Signals are plotted as percentage of input for precipitation with pol II (8WG16) antibody. The data shown are representative of a duplicate. (**E**) cDNA was prepared from HeLa tk⁻ cells transfected with siRNA targeting BTAF1 or control siRNA. mRNA levels of *RPL31*, *RPL34*, *H2A*, *H2B*, *GAPDH* and *BTAF1* were analyzed by quantitative PCR. Depicted is an average of three biological independent experiments. (**F**) Protein levels were analyzed in total lysates of the transfected cells as described in B by immunoblotting with BTAF1, TBP, NC2α and tubulin antibodies.

observation that only DNA-bound TBP is a substrate for NC2. Our experiments in yeast (van Werven et al., 2008) combined with other studies (Meisterernst et al., 1991; Inostroza et al., 1992) indicate that this complex is transcriptionally inactive. Our data suggest that the immobilized TBP is locked in an NC2 complex. It has been proposed that TBP-NC2 slides along the DNA fibre (Schluesche et al., 2007). This sliding of the transcriptionally inactive NC2-TBP complex (Schluesche et al., 2007) could clear the core promoter for formation of a functional preinitiation complex. This is supported by the ChIP analysis (Fig. 6), which showed an increased NC2α occupancy on promoters upon BTAF1 knockdown. Although NC2α binding is increased around the transcription start site, this does not affect transcription as shown by the pol II ChIP and RT-PCR analysis. Consistent with this is the observation that ChIP experiments with *mot1* mutant cells show an increased TBP and NC2 association at a specific set of promoters (Dasgupta et al., 2005; Geisberg et al., 2002), as observed in the ChIP experiments under BTAF1 knockdown conditions (Fig. 6). These observations suggest co-occurrence of NC2-TBP repressive complexes and TBP in functional transcription complex on the same chromatin fragment. We propose that NC2-TBP slides away from the core promoter and does not obstruct association of active transcription complexes.

In general, several studies now indicate that basal transcription factor complexes are highly dynamic in vivo (Darzacq et al., 2007; Hager et al., 2009; Hoogstraten et al., 2002; Sprouse et al., 2008; van Werven et al., 2009). In addition, it has been shown that many gene-specific transcription factors have relative short DNA residence times (Bosisio et al., 2006; Farla et al., 2004; McNally et al., 2000; Mueller et al., 2008; Muller et al., 2001). We now report that TFIID-TAFs are also mobile and display short residence times on chromosomal DNA of 1-2 seconds (Fig. 1C). Although a fraction of TBP is bound to chromatin with a relative long residence time, most of TBP (~70%) is freely mobile. Together, our results add to previously published observations (Darzacq et al., 2007) and further suggest that the pol II PICs are very dynamic structures and that TBP bound to pol II promoters is rapidly exchanging (van Werven et al., 2009). This challenges models of pol II mRNA factories consisting of tightly bound and rather immobile protein assemblies (Sutherland and Bickmore, 2009), but rather support a model where transcription sites are rapidly assembling and disassembling entities (Lebedeva et al., 2005). Importantly, this kinetic model allows for a rapid response to changes in mRNA requirement of cells. Furthermore, the antagonistic regulation of TBP-chromatin interactions by BTAF1 and NC2 fits to models of transcriptional bursts (Chubb et al., 2006) in which promoters can switch rapidly between transcriptionally active and inactive states. We propose that this switching is intimately linked to NC2 and BTAF1 regulation of TBP dynamics.

Materials and Methods

Antibodies

The monoclonal TBP antibody 1F8, the rabbit polyclonal antibody PF299 and the mouse polyclonal antibodies C-BTAF1 (blanc-o and L.O.R.O.) against BTAF1 have been described previously (Pereira et al., 2004). The monoclonal TBP antibodies

SL30 (Ruppert et al., 1996), NC2α antibodies 4G7 (Gilfillan et al., 2005) and polyclonal TAF5 antibody (Christova and Oelgeschlager, 2002) have been described. The monoclonal GFP antibody (mix of clones 7.1 and 13.1) was from Roche Applied Science and the monoclonal tubulin antibody (DM1A) was obtained from Calbiochem. Histone H4 (ab31827) and TAF1 (6B3) antibodies were obtained from Abcam and Upstate, respectively. GAPDH antibodies (6C5) were obtained from Millipore. The monoclonal HA antibody was purified from the hybridoma cell line 12CA5 (ATTC).

DNA constructs

The constructs pEGFP-TBP, pTER, pCAG-TR^s and pcDNA4-TO luciferase (Chen et al., 2002; van de Wetering et al., 2003) have been described previously. To generate a retroviral expression vector for N-terminal or C-terminal fusion proteins, the GFP ORF was amplified by PCR and inserted into the pBabe puro plasmid, resulting in pBabe-puro GFP-N-term and pBabe-puro GFP C-term. The plasmids were modified to act as Gateway destination plasmids by introducing a blunt-ended cassette containing *attR* sites flanking the *ccdB* gene and the chloramphenicol resistance gene from RfC (for the N-terminal fusion construct) or RfA (for the C-terminal fusion construct) resulting in pBabe-puro GFP-Nterm Dest GW and pBabe-puro GFP-Cterm Dest GW, respectively. The cloning junctions were verified by DNA sequencing.

Human TBP, TAF1, TAF5, NC2α, NC2β, BTAF1 and Histone H2B were amplified using appropriate oligonuclotides flanked with *attB1* or *attB2* sequences. The amplified sequences was cloned into pDONR201 (Invitrogen) using a standard BP reaction to generate pENTR-N-TBP, pENTR-N-TAF1, pENTR-N-TAF5, pENTR-N-NC2α, pENTR-N-NC2β, pENTR-N-BTAF1 and pENTR-C-H2B, respectively. pBabe GFP-TBP, pBabe GFP-TAF1, pBabe GFP-TAF5, pBabe GFP-NC2α and pBabe GFP-NC2β were generated in a LR reaction with pBabe puro GFP-Nterm Dest GW and, respectively, pENTR-N-TBP, pENTR-N-TAF1, pENTR-N-TAF5, pENTR-N-NC2α and pENTR-N-NC2β. pBabe H2B-GFP was generated in a LR reaction with pBabe puro GFP-Cterm Dest GW and pENTR-C-H2B. pBabe NLS-GFP was generated by conventional cloning of an oligonucleotide encoding an optimal translational initiation site followed by the SV40 NLS (PKKKRKV) in pBabe-puro GFP-C-term. NC2α and NC2β were amplified using appropriate oligonucleotides flanked with restriction sites and inserted into, respectively, pcDNA3.1 HA and pcDNA3.1 Flag by conventional cloning to obtain pCMV HA NC2α and pCMV Flag NC2β. pMT2-SM HA was modified to act as a destination plasmid by introducing the RfC cassette to yield pMT2-SM HA Dest GW. To yield the mammalian expression constructs, pMT2-SM HA-BTAF1 and pMT2-SM HA TBP pMT2-SM HA Dest GW was recombined in a standard LR reaction with either pENTR-N-BTAF1 or pENTR-N-TBPwt.

pTER shBTAF1 constructs were generated by inserting an dsDNA-oligo encoding a RNA short hairpin targeting knock-down of BTAF1 into the *Bgl*II/*Hin*dIII sites of the pTER vector (van de Wetering et al., 2003). Sequences of used oligonucleotides are available upon request.

Cell lines and transient transfection

HeLa tk$^-$, U2OS and HEK293T cells were grown in Dulbecco's modified Eagle's medium (DMEM) supplemented with 10% foetal calf serum, L-glutamine and antibiotics at 37°C. Mutant hamster ts13 cells (Sekiguchi et al., 1991) were grown in DMEM with high glucose (4.5 mg/ml) supplemented with 10% foetal calf serum, L-glutamine and antibiotics at 34°C or 39.5°C. Transient transfection of plasmid DNA was performed 6 hours after seeding using FuGene6 transfection reagent according to the manufacturer's instructions (Roche Applied Science). Transient siRNA transfection was performed 18-24 hours after seeding using Dharmafect 1 reagent (Dharmacon). siGLO Red Transfection Indicator (D-001630-02, Dharmacon) was included in the siRNA transfection and revealed a transfection efficiency of at least 95% (supplementary material Fig. S3).

Generation of stable cell lines

pBabe constructs were used to generate retrovirus particles using the Phoenix ecotropic packaging cells. HeLa or U2OS target cells were electroporated with an expression plasmid for the ecotropic receptor 24 hours before infection. For infection, cells were exposed to a 1:1 dilution of virus supernatant and fresh medium in presence of polybrene (5 μg/ml). Infected cells were split 24 hours after infection and subjected to puromycin selection (0.5 mg/l for HeLa, 1.0 mg/l for U2OS). Monoclonal colonies were isolated, propagated and tested for expression both by fluorescent microscopy and immunoblot analysis.

The Tet repressor expressing construct pCAG-TR^s was transfected in U2OS and HeLa cells using the calcium phosphate method. Hygromycin-resistant clones were tested by transient transfection of the luciferase construct TO Luc as described (van de Wetering et al., 2003). HeLa TR^s A7 and U2OS TR^s C2.1 were used to generate BTAF1 inducible knock-down cell lines by transfecting pTER shBTAF1 using Dharmafect reagent 1 according to the manufacturer (Dharmacon). Cells were selected using zeocin and hygromycin. Individual clones were isolated and tested for efficient knockdown of BTAF1. After transient transfection of the ecotropic receptor BTAF1, knock-down cell lines were infected with retroviruses expressing GFP-TBP, NLS-GFP or H2B-GFP as described above.

Immunoprecipitation and immunoblotting

Cells were lysed in IP lysis buffer [50 mM Tris-HCl (pH 8.0), 150 mM KCl, 5 mM $MgCl_2$, 0.5 mM EDTA, 0.1% NP40, 10% glycerol and protease inhibitors]. Cleared lysate was added to antibody-coupled protein A beads (anti-BTAF1 Pf299) or Dynabeads Sheep-anti-mouse (GFP antibody or anti-TBP SL30). Precipitated proteins were separated on 10% SDS-PAGE and blotted onto PVDF membranes. The membrane was developed with the appropriate antibodies and ECL (Pierce).

Gel filtration

Nuclear extract was prepared from HeLa GFP-TBP cell lines as described (Dignam et al., 1983) and dialysed against buffer A [20 mM HEPES-KOH (pH 7.9), 20% glycerol, 1 mM EDTA, 1 mM DTT, 1 mM PMSF, 400 mM KCl, 0.1% Triton X-100]. Nuclear extract was applied on a Superose 12 column and eluted with buffer A. Aliquots of the 0.4 ml fractions were separated on a 10% SDS-polyacrylamide gel and analyzed by immunoblotting.

Strip-FRAP

Cell imaging and FRAP studies were performed using a Zeiss 510 META confocal LSM using the 488 nm laser line of a 200 mW Argon laser with tube current set at 6.1-6.3 A. All images and FRAP results were obtained using a 40× oil immersion lens (NA=1.3) using filters that pass emission light between 505 and 530 nm. Strip-FRAP was performed as described (Farla et al., 2004; van Royen et al., 2009). Briefly, a narrow strip (~0.75 μm) spanning the width of the nucleus was monitored every 21 ms using 0.2-0.5% laser power of the 488 nm laser line, an intensity at which no significant monitor bleaching was observed. After 4 seconds the strip was quickly bleached for 42 mseconds at maximum laser power. Subsequently, recovery of fluorescence was monitored at 21 ms intervals for 40 seconds. For quantitative analyses, fluorescence intensity in the strip was expressed relatively to the fluorescence before bleaching. For each protein the average of 10 nuclei were taken.

Quantitative FRAP analysis

Computer modelling used to generate FRAP curves for fitting was based on Monte Carlo simulation of diffusion and binding to immobile elements (representing chromatin binding) in an ellipsoidal volume (representing the nucleus) (Farla et al., 2004; Farla et al., 2005; Xouri et al., 2007). Bleaching simulation was based on experimentally derived three-dimensional laser intensity profiles, which determined the probability for each molecule to become bleached considering their 3D position relative to the laser beam. Diffusion was simulated at each new time step $t + \Delta t$ by deriving a new position ($x_{t+\Delta t}$, $y_{t+\Delta t}$, $z_{t+\Delta t}$) for all mobile molecules from their current position (x_t, y_t, z_t) by $x_{t+\Delta t}=x_t + G(r_1)$, $y_{t+\Delta t}=y_t + G(r_2)$, and $z_{t+\Delta t}=z_t + G(r_3)$, where r_i is a random number ($0 \leq r_i \leq 1$) chosen from a uniform distribution, and $G(r_i)$ is an inversed cumulative Gaussian distribution with $\mu=0$ and $\sigma^2=2D\Delta t$, where D is the diffusion coefficient. Immobilization was derived from simple binding kinetics: $k_{on}/k_{off}=F_{imm} / (1–F_{imm})$, where F_{imm} is the fraction of immobile molecules. The probability per unit time to be released from the immobile state was given by $P_{mobilise}=k_{off}=1 / T_{imm}$, where T_{imm} is the characteristic time spent in immobile complexes expressed in unit time steps. The probability per unit time for each mobile particle to become immobilized (representing chromatin-binding) was defined as $P_{immobilise}=k_{on}=k_{off} \cdot F_{imm} / (1–F_{imm})$, where $k_{off}=1 / T_{imm}$. Note that k_{on} and k_{off} in this model are effective rate constants with dimension s^{-1}.

In all simulations, the size of the ellipsoid was based on the size of the measured nuclei, and the region used in the measurements determined the size of the simulated bleach region. The laser intensity profile using the simulation of the bleaching step was derived from confocal images stacks of chemically fixed nuclei containing GFP that were exposed to a stationary laser beam at various intensities and varying exposure times. The unit time step Δt corresponded to the experimental sample rate of 21 mseconds.

For quantitative analysis of the FRAP data, raw FRAP curves were normalized to pre-bleach values and the best fitting curves (by ordinary least squares) were selected from a large set of computer simulated FRAP curves in which three parameters representing mobility properties were varied: diffusion rate (ranging from 0.04 to 25 $\mu m^2/s$), immobile fraction (0, 10, 20, …, 90%) and time spent in immobile state (2, 4, 8, 16, 32, 64, 128, 256, 512, 1024, ∞ s). Because individual curves generated by Monte Carlo modelling, in contrast to analytically derived curves, show the slight variation typical for diffusion of a limited amount of molecules in a small volume (i.e. the exact, relatively small number of molecules in a small volume varies, a phenomenon on which, for example, fluorescence correlation spectroscopy is based), we did not use the best-fitting curve only, but took the ten best-fitting curves and calculated the average diffusion coefficients and rate constants corresponding to these curves.

Chromatin isolation

HeLa TR^s shBTAF1 cells were grown for 8 days with or without doxycycline (1 mg/l). Cells were trypsinised and resuspended in hypotonic lysis buffer [10 mM HEPES-KOH (pH 8.0), 1.5 mM $MgCl_2$, 10 mM KCl, 0.5 mM DTT and 0.5 mM PMSF]. Cells were lysed using a 27G syringe. One volume of 2× whole cell extraction buffer was added [40 mM HEPES-KOH (pH 8.0), 1.5 mM $MgCl_2$, 4 mM EDTA, 50% glycerol, 1.2 M NaCl, 0.5 mM DTT and protease inhibitors] and lysates were tumbled for 30 minutes at 4°C followed by centrifugation for 45 minutes at

90,000 ***g*** (TLA100.2) to yield the soluble fraction. High salt buffer [20 mM HEPES-KOH (pH 7.9), 600 mM NaCl, 340 mM sucrose, 0.1% Triton X-100, 1 mM EDTA and 1 mM β-mercaptoethanol] was added to the pellet. Samples were homogenized and tumbled for 30 minutes at 4°C followed by centrifugation for 30 minutes at 90,000 ***g*** to yield wash 1. This wash was repeated a second time (wash 2). One pellet volume of nucleosome isolation buffer [20 mM HEPES-KOH (pH 7.9), 250 mM sucrose, 10 mM $MgCl_2$, 3 mM $CaCl_2$, 0.1% Triton X-100 and 5 mM β-mercaptoethanol] was added to the pellet. Samples were prewarmed for 5 minutes at 37°C. Micrococcal nuclease (10 U/ml) was added and the samples were incubated for an additional 30 minutes at 37°C. Reaction was stopped with 10 mM EGTA and cooled on ice. Soluble chromatin fraction was isolated by centrifugation for 5 minutes at 10,000 ***g*** in a table top centrifuge.

Chromatin immunoprecipitation

Subconfluent cultures of HeLa tk^- cells were crosslinked by addition of 1% formaldehyde in PBS for 10 minutes at 37°C. Cells were lysed in buffer [50 mM Tris-HCl (pH 7.9), 1% SDS, 10 mM EDTA, 1 mM DTT, and protease inhibitors]. The lysate was sonicated six times for 30 seconds in a Bioruptor (Diagenode, Belgium) resulting in DNA fragments of 200 to 600 bp. Soluble material was supplemented with 0.1% Triton X-100 and 0.1% Na-DOC and incubated for 6 hours with Dynabeads coupled to antibody of interest. Samples were processed as previously described (Vermeulen et al., 2007). Binding to promoter and ORF regions of *RPL31, RPL34*, *RPS10* and *H2BJ-H2AG* locus DNA was measured by quantitative PCR (Chromo4-equipped PCR cycler 5MJ Research, Bio-Rad) and normalized against input samples from the same experiment. Primer sequences are available upon request.

Gene expression analysis

Total RNA was extracted using the RNeasy kit (Qiagen) including a DNase treatment step. Total RNA (250 ng) was used for cDNA synthesis (Superscript II, Invitrogen). Expression of *RPL31*, *RPL34*, *RPS10*, *H2B*, *H2A*, *BTAF1* and *GAPDH* were analyzed by quantitative PCR and normalized against a standard reference cDNA from untreated HeLa tk^- cells.

We thank M. Meisterernst, I. Davidson, N. Hernandez, H. Stunnenberg and T. Oelgeschlager for antibodies; M. van de Wetering and D. Chen for plasmids; L. Kleij and H.A.A.M. van Teeffelen for technical assistance; Folkert van Werven, Pim Pijnappel and Markus Kleinschmidt for critically reading of the manuscript; and the Timmers group for valuable discussions. This work was supported by grants from the European community (STREP LSHG-CT-2004-502950; HPRN-CT 00504228 and EUTRACC LSHG-CT-2007-037445), the Netherlands Organization for Scientific research (ALW 855.01.077/03-DYNA-F-03 and CW 700.57.302), the Netherlands Proteomics Center, ANR (05-BLAN-0396-01; Regulome), INCA (2008-UBICAN), AICR (09-0258) and by the Human Frontier Science Program (LT-0860/2005).

Supplementary material available online at
http://jcs.biologists.org/cgi/content/full/123/15/2663/DC1

References

Boireau, S., Maiuri, P., Basyuk, E., de la Mata, M., Knezevich, A., Pradet-Balade, B., Backer, V., Kornblihtt, A., Marcello, A. and Bertrand, E. (2007). The transcriptional cycle of HIV-1 in real-time and live cells. *J. Cell Biol.* **179**, 291-304.

Bosisio, D., Marazzi, I., Agresti, A., Shimizu, N., Bianchi, M. E. and Natoli, G. (2006). A hyper-dynamic equilibrium between promoter-bound and nucleoplasmic dimers controls NF-kappaB-dependent gene activity. *EMBO J.* **25**, 798-810.

Burley, S. K. and Roeder, R. G. (1996). Biochemistry and structural biology of transcription factor IID (TFIID). *Annu. Rev. Biochem.* **65**, 769-799.

Chen, D., Hinkley, C. S., Henry, R. W. and Huang, S. (2002). TBP dynamics in living human cells: constitutive association of TBP with mitotic chromosomes. *Mol. Biol. Cell* **13**, 276-284.

Christova, R. and Oelgeschlager, T. (2002). Association of human TFIID-promoter complexes with silenced mitotic chromatin in vivo. *Nat. Cell Biol.* **4**, 79-82.

Chubb, J. R., Trcek, T., Shenoy, S. M. and Singer, R. H. (2006). Transcriptional pulsing of a developmental gene. *Curr. Biol.* **16**, 1018-1025.

Cler, E., Papai, G., Schultz, P. and Davidson, I. (2009). Recent advances in understanding the structure and function of general transcription factor TFIID. *Cell. Mol. Life Sci.* **66**, 2123-2134.

Core, L. J. and Lis, J. T. (2008). Transcription regulation through promoter-proximal pausing of RNA polymerase II. *Science* **319**, 1791-1792.

Darzacq, X., Shav-Tal, Y., de Turris, V., Brody, Y., Shenoy, S. M., Phair, R. D. and Singer, R. H. (2007). In vivo dynamics of RNA polymerase II transcription. *Nat. Struct. Mol. Biol.* **14**, 796-806.

Dasgupta, A., Juedes, S. A., Sprouse, R. O. and Auble, D. T. (2005). Mot1-mediated control of transcription complex assembly and activity. *EMBO J.* **24**, 1717-1729.

Dignam, J. D., Lebovitz, R. M. and Roeder, R. G. (1983). Accurate transcription initiation by RNA polymerase II in a soluble extract from isolated mammalian nuclei. *Nucleic Acids Res.* **11**, 1475-1489.

Dundr, M., Hoffmann-Rohrer, U., Hu, Q., Grummt, I., Rothblum, L. I., Phair, R. D. and Misteli, T. (2002). A kinetic framework for a mammalian RNA polymerase in vivo. *Science* **298**, 1623-1626.

Farla, P., Hersmus, R., Geverts, B., Mari, P. O., Nigg, A. L., Dubbink, H. J., Trapman, J. and Houtsmuller, A. B. (2004). The androgen receptor ligand-binding domain stabilizes DNA binding in living cells. *J. Struct. Biol.* **147**, 50-61.

Farla, P., Hersmus, R., Trapman, J. and Houtsmuller, A. B. (2005). Antiandrogens prevent stable DNA-binding of the androgen receptor. *J. Cell Sci.* **118**, 4187-4198.

Geisberg, J. V., Moqtaderi, Z., Kuras, L. and Struhl, K. (2002). Mot1 associates with transcriptionally active promoters and inhibits association of NC2 in Saccharomyces cerevisiae. *Mol. Cell. Biol.* **22**, 8122-8134.

Gilfillan, S., Stelzer, G., Piaia, E., Hofmann, M. G. and Meisterernst, M. (2005). Efficient binding of NC2.TATA-binding protein to DNA in the absence of TATA. *J. Biol. Chem.* **280**, 6222-6230.

Goppelt, A., Stelzer, G., Lottspeich, F. and Meisterernst, M. (1996). A mechanism for repression of class II gene transcription through specific binding of NC2 to TBP-promoter complexes via heterodimeric histone fold domains. *EMBO J.* **15**, 3105-3116.

Gorski, S. A., Snyder, S. K., John, S., Grummt, I. and Misteli, T. (2008). Modulation of RNA polymerase assembly dynamics in transcriptional regulation. *Mol. Cell* **30**, 486-497.

Hager, G. L., McNally, J. G. and Misteli, T. (2009). Transcription dynamics. *Mol. Cell* **35**, 741-753.

Hoogstraten, D., Nigg, A. L., Heath, H., Mullenders, L. H., van Driel, R., Hoeijmakers, J. H., Vermeulen, W. and Houtsmuller, A. B. (2002). Rapid switching of TFIIH between RNA polymerase I and II transcription and DNA repair in vivo. *Mol. Cell* **10**, 1163-1174.

Hsu, J. Y., Juven-Gershon, T., Marr, M. T., 2nd, Wright, K. J., Tjian, R. and Kadonaga, J. T. (2008). TBP, Mot1, and NC2 establish a regulatory circuit that controls DPE-dependent versus TATA-dependent transcription. *Genes Dev.* **22**, 2353-2358.

Inostroza, J. A., Mermelstein, F. H., Ha, I., Lane, W. S. and Reinberg, D. (1992). Dr1, a TATA-binding protein-associated phosphoprotein and inhibitor of class II gene transcription. *Cell* **70**, 477-489.

Johannes, F., Wardenaar, R., Colome-Tatche, M., Mousson, F., de Graaf, P., Mokry, M., Guryev, V., Timmers, H. T., Cuppen, E. and Jansen, R. C. (2010). Comparing genome-wide chromatin profiles using ChIP-chip or ChIP-seq. *Bioinformatics* **26**, 1000-1006.

Karpova, T. S., Kim, M. J., Spriet, C., Nalley, K., Stasevich, T. J., Kherrouche, Z., Heliot, L. and McNally, J. G. (2008). Concurrent fast and slow cycling of a transcriptional activator at an endogenous promoter. *Science* **319**, 466-469.

Kieffer-Kwon, P., Martianov, I. and Davidson, I. (2004). Cell-specific nucleolar localization of TBP-related factor 2. *Mol. Biol. Cell* **15**, 4356-4368.

Kimura, H., Sugaya, K. and Cook, P. R. (2002). The transcription cycle of RNA polymerase II in living cells. *J. Cell Biol.* **159**, 777-782.

Klejman, M. P., Pereira, L. A., van Zeeburg, H. J., Gilfillan, S., Meisterernst, M. and Timmers, H. T. (2004). NC2alpha interacts with BTAF1 and stimulates its ATP-dependent association with TATA-binding protein. *Mol. Cell. Biol.* **24**, 10072-10082.

Lebedeva, L. A., Nabirochkina, E. N., Kurshakova, M. M., Robert, F., Krasnov, A. N., Evgen'ev, M. B., Kadonaga, J. T., Georgieva, S. G. and Tora, L. (2005). Occupancy of the Drosophila hsp70 promoter by a subset of basal transcription factors diminishes upon transcriptional activation. *Proc. Natl. Acad. Sci. USA* **102**, 18087-18092.

Leurent, C., Sanders, S. L., Demeny, M. A., Garbett, K. A., Ruhlmann, C., Weil, P. A., Tora, L. and Schultz, P. (2004). Mapping key functional sites within yeast TFIID. *EMBO J.* **23**, 719-727.

McNally, J. G., Muller, W. G., Walker, D., Wolford, R. and Hager, G. L. (2000). The glucocorticoid receptor: rapid exchange with regulatory sites in living cells. *Science* **287**, 1262-1265.

Meisterernst, M., Roy, A. L., Lieu, H. M. and Roeder, R. G. (1991). Activation of class II gene transcription by regulatory factors is potentiated by a novel activity. *Cell* **66**, 981-993.

Mousson, F., Kolkman, A., Pijnappel, W. W., Timmers, H. T. and Heck, A. J. (2008). Quantitative proteomics reveals regulation of dynamic components within TATA-binding protein (TBP) transcription complexes. *Mol. Cell Proteomics* **7**, 845-852.

Mueller, F., Wach, P. and McNally, J. G. (2008). Evidence for a common mode of transcription factor interaction with chromatin as revealed by improved quantitative fluorescence recovery after photobleaching. *Biophys. J.* **94**, 3323-3339.

Muller, F., Demeny, M. A. and Tora, L. (2007). New problems in RNA polymerase II transcription initiation: matching the diversity of core promoters with a variety of promoter recognition factors. *J. Biol. Chem.* **282**, 14685-14689.

Muller, W. G., Walker, D., Hager, G. L. and McNally, J. G. (2001). Large-scale chromatin decondensation and recondensation regulated by transcription from a natural promoter. *J. Cell Biol.* **154**, 33-48.

Pereira, L. A., Klejman, M. P. and Timmers, H. T. (2003). Roles for BTAF1 and Mot1p in dynamics of TATA-binding protein and regulation of RNA polymerase II transcription. *Gene* **315**, 1-13.

Pereira, L. A., Klejman, M. P., Ruhlmann, C., Kavelaars, F., Oulad-Abdelghani, M., Timmers, H. T. and Schultz, P. (2004). Molecular architecture of the basal transcription factor B-TFIID. *J. Biol. Chem.* **279**, 21802-21807.

Ruppert, S. M., McCulloch, V., Meyer, M., Bautista, C., Falkowski, M., Stunnenberg, H. G. and Hernandez, N. (1996). Monoclonal antibodies directed against the amino-

terminal domain of human TBP cross-react with TBP from other species. *Hybridoma* **15**, 55-68.

Schluesche, P., Stelzer, G., Piaia, E., Lamb, D. C. and Meisterernst, M. (2007). NC2 mobilizes TBP on core promoter TATA boxes. *Nat. Struct. Mol. Biol.* **14**, 1196-1201.

Sekiguchi, T., Nohiro, Y., Nakamura, Y., Hisamoto, N. and Nishimoto, T. (1991). The human CCG1 gene, essential for progression of the G1 phase, encodes a 210-kilodalton nuclear DNA-binding protein. *Mol. Cell. Biol.* **11**, 3317-3325.

Sikorski, T. W. and Buratowski, S. (2009). The basal initiation machinery: beyond the general transcription factors. *Curr. Opin. Cell Biol.* **21**, 344-351.

Sprouse, R. O., Karpova, T. S., Mueller, F., Dasgupta, A., McNally, J. G. and Auble, D. T. (2008). Regulation of TATA-binding protein dynamics in living yeast cells. *Proc. Natl. Acad. Sci. USA* **105**, 13304-13308.

Stenoien, D. L., Patel, K., Mancini, M. G., Dutertre, M., Smith, C. L., O'Malley, B. W. and Mancini, M. A. (2001). FRAP reveals that mobility of oestrogen receptor-alpha is ligand- and proteasome-dependent. *Nat. Cell Biol.* **3**, 15-23.

Sutherland, H. and Bickmore, W. A. (2009). Transcription factories: gene expression in unions? *Nat. Rev. Genet.* **10**, 457-466.

Takada, R., Nakatani, Y., Hoffmann, A., Kokubo, T., Hasegawa, S., Roeder, R. G. and Horikoshi, M. (1992). Identification of human TFIID components and direct interaction between a 250-kDa polypeptide and the TATA box-binding protein (TFIID tau). *Proc. Natl. Acad. Sci. USA* **89**, 11809-11813.

Thomas, M. C. and Chiang, C. M. (2006). The general transcription machinery and general cofactors. *Crit. Rev. Biochem. Mol. Biol.* **41**, 105-178.

Timmers, H. T., Meyers, R. E. and Sharp, P. A. (1992). Composition of transcription factor B-TFIID. *Proc. Natl. Acad. Sci. USA* **89**, 8140-8144.

Tora, L. (1992). A unified nomenclature for TATA box binding protein (TBP)-associated factors (TAFs) involved in RNA polymerase II transcription. *Genes Dev.* **16**, 673-675.

van de Wetering, M., Oving, I., Muncan, V., Pon Fong, M. T., Brantjes, H., van Leenen, D., Holstege, F. C., Brummelkamp, T. R., Agami, R. and Clevers, H. (2003). Specific inhibition of gene expression using a stably integrated, inducible small-interfering-RNA vector. *EMBO Rep.* **4**, 609-615.

van Royen, M. E., Farla, P., Mattern, K. A., Geverts, B., Trapman, J. and Houtsmuller, A. B. (2009). Fluorescence recovery after photobleaching (FRAP) to study nuclear protein dynamics in living cells. *Methods Mol. Biol.* **464**, 363-385.

van Werven, F. J., van Bakel, H., van Teeffelen, H. A., Altenaar, A. F., Groot Koerkamp, M. G., Heck, A. J., Holstege, F. C. and Timmers, H. T. (2008). Cooperative action of NC2 and Mot1p to regulate TATA-binding protein function across the genome. *Genes Dev.* **22**, 2359-2369.

van Werven, F. J., van Teeffelen, H. A., Holstege, F. C. and Timmers, H. T. (2009). Distinct promoter dynamics of the basal transcription factor TBP across the yeast genome. *Nat. Struct. Mol. Biol.* **16**, 1043-1048.

Vermeulen, M., Mulder, K. W., Denissov, S., Pijnappel, W. W., van Schaik, F. M., Varier, R. A., Baltissen, M. P., Stunnenberg, H. G., Mann, M. and Timmers, H. T. (2007). Selective anchoring of TFIID to nucleosomes by trimethylation of histone H3 lysine 4. *Cell* **131**, 58-69.

Xouri, G., Squire, A., Dimaki, M., Geverts, B., Verveer, P. J., Taraviras, S., Nishitani, H., Houtsmuller, A. B., Bastiaens, P. I. and Lygerou, Z. (2007). Cdt1 associates dynamically with chromatin throughout G1 and recruits Geminin onto chromatin. *EMBO J.* **26**, 1303-1314.

Yao, J., Munson, K. M., Webb, W. W. and Lis, J. T. (2006). Dynamics of heat shock factor association with native gene loci in living cells. *Nature* **442**, 1050-1053.

Yao, J., Ardehali, M. B., Fecko, C. J., Webb, W. W. and Lis, J. T. (2007). Intranuclear distribution and local dynamics of RNA polymerase II during transcription activation. *Mol. Cell* **28**, 978-990.